crystals

MDPI

*Article*

# The Hydrothermal Method of Preparing Boron–Saccharide Precursors for the Synthesis of Boron Carbide and Its Influence on the Morphology and Phase Composition of the Obtained Products

**Dawid Kozień *, Katarzyna Pasiut, Wojciech Banaś, Mateusz Zagórny and Janusz Partyka ***

Department of Ceramics and Refractories, Faculty of Materials Science and Ceramics, AGH University of Krakow, Mickiewicza, 30-059 Krakow, Poland; kpasiut@agh.edu.pl (K.P.); wbanas@student.agh.edu.pl (W.B.); mzagorny13@poczta.fm (M.Z.)

* Correspondence: kozien@agh.edu.pl (D.K.); partyka@agh.edu.pl (J.P.)

**Abstract:** Owing to its properties, boron carbide has been applied in scientific and industrial fields. For this reason, $B_4C$ powders should be characterized by high purity and homogeneity in grain size and shape. In this study, boron carbide was prepared using precursors obtained using a hydrothermal method, and the grain morphology of the product was investigated. Boric acid and the saccharides glucose, fructose, inulin, and sorbitol were used as the precursors. Two precursor dehydration methods, freeze-drying and recrystallization, were compared. The precursors were subjected to DLS grain size and FT-IR spectrophotometric studies, and SEM observations of the precursors and products were performed, confirming that boron carbide powders could be successfully synthesized.

**Keywords:** boron carbide; nanopowders; hydrothermal method; saccharides

check for updates

**Citation:** Kozień, D.; Pasiut, K.; Banaś, W.; Zagórny, M.; Partyka, J. The Hydrothermal Method of Preparing Boron–Saccharide Precursors for the Synthesis of Boron Carbide and Its Influence on the Morphology and Phase Composition of the Obtained Products. *Crystals* **2024**, *14*, 153. https://doi.org/10.3390/cryst14020153

Academic Editor: Weichao Bao

Received: 22 December 2023
Revised: 24 January 2024
Accepted: 26 January 2024
Published: 31 January 2024

**Copyright:** © 2024 by the authors. Licensee MDPI, Basel, Switzerland. This article is an open access article distributed under the terms and conditions of the Creative Commons Attribution (CC BY) license (https://creativecommons.org/licenses/by/4.0/).

## 1. Introduction

Owing to its specific properties, boron carbide ($B_4C$) has numerous applications in various industries. Applications, such as in abrasives, cutting tool components, and nozzles, are based on the remarkable abrasion resistance of this compound. It slow density (2.52 g/cm$^3$) [1] combined with its high hardness (over 30 GPa) [1–4] allows boron carbide to be used as armor plates in ballistic applications. The material is also characterized by a wide active cross-section for thermal neutron capture (755 b) [5], making it the best material for the construction of neutron diodes. This property also allows $B_4C$ to be considered a candidate for the role of a boron carrier in boron neutron capture therapy (BNCT) [6,7]. This medical application requires powders with well-defined morphology and purity. The commercial method of producing boron carbide-carbothermic reduction [5,7–9] in Acheson furnaces does not allow for precise control of the parameters described, whereas synthesis from free elements is associated with high costs related to the price of elemental boron. For this reason, research is needed on alternative methods of synthesizing $B_4C$, which include synthesis where the carbon source is a substance of organic origin; the most promising method appears to be hydrothermal.

Hydrothermal synthesis is one of the most widely used methods for producing nanomaterials. Its origin dates back to the mid-19th century, when quartz was synthesized in the form of micrometer-sized crystallites, followed by barium ($BaCO_3$) and strontium ($SrCO_3$) carbonates at 200 °C and 15 bar [10]. It is described as a wet bottom-up synthesis method, proceeding in sealed reactors at temperatures of 100–1000 °C, under elevated pressures of 1–100 MPa. Reactions occur in either polar or nonpolar solvents, which are in subcritical (temperatures lower than 240 °C) or supercritical (above 240 °C, high-pressure) states. The main difference between synthesis under hydrothermal conditions and solid-phase synthesis is the reactivity, which is due to different reaction mechanisms. Examples of inorganic

materials produced via hydrothermal synthesis include optical materials ($AlPO_4$) [11], laser crystals ($LiTaO_3$) [12], oxide materials ($ZnO_2$ and $GeO_2$) [12–14], ferroelectric, magnetoelectric, and photoelectric materials, superconducting membranes, artificial crystals, and quartz monocrystals [15]. The appearance, operation, and modifications of the apparatuses used in the hydrothermal method have been described extensively in the literature [2,3].

Owing to the high demand for high-purity boron carbide, much research is currently being conducted to develop methods for synthesizing such compounds. Current research trends focus on synthesizing powders from natural precursors such as saccharides [13–17], cotton [18], and aloe vera [19]. The synthesis of saccharides and boric acid using a hydrothermal method has already been investigated by Sudoh [20]; however, current scientific developments allow for refinement and further development. Because of their structure (based on carbon and hydrogen), organic compounds appear to be an ideal carbon source, and because of their popularity and low price (compared to analogous inorganic carbon sources), they seem to be promising precursors for this type of synthesis reaction. The hydrothermal synthesis method makes it possible to reduce the grain size of the saccharide precursors and control the morphology of the powder produced. A study was conducted in which spherical carbon structures were obtained by subjecting fructose to hydrothermal conditions. The obtained spheres consisted of nanoparticle aggregates. The formation mechanism of the final product was described as a three-step process. In the first step, fructose is dehydrated to hydroxymethylfurfural (HMF) [21], an organic chemical compound belonging to the alcohol and aldehyde groups that contains a five-membered furan ring. Owing to the presence of active functional groups in the HMF structure, its polycondensation, the second step in the carbon sphere formation process, is possible. In the third stage, the nanoparticles aggregate to form larger carbon structures. The final product was a product of HMF condensation, and the analysis did not reveal the presence of the structural characteristics of fructose. Analogous studies on other saccharides outside the ketose group have shown similar results. The authors described the mechanism of these reactions as dehydration combined with ring opening, breaking carbon–carbon bonds, followed by processes such as polymerization, polycondensation, aromatization, or keto–enol tautomerism.

Hydrothermal synthesis is one of the most widely used methods for producing nanomaterials, which is described as a wet bottom-up synthesis that occurs in sealed reactors at elevated temperatures and pressures. There are a huge number of reports on hydrothermal synthesis in the modern literature [11,14,19,22,23]. The innovation proposed in this article does not involve changes to the method itself, but it allows the use of a hydrothermal method to obtain boron and carbon sources from cheap and readily available precursors—boric acid as a boron source and saccharides (and their derivatives) as carbon sources [24,25].

## 2. Materials and Methods

To produce precursors for the synthesis of boron carbide using the hydrothermal method, mixtures consisting of boron sources (boric acid $H_3BO_3$) and carbon sources (mono and polysaccharides) were used. To compare the influence of saccharide structure on the mechanism of carbon sphere formation, the following compounds were selected: fructose (ketose), glucose (aldose), inulin (polyketose), and sorbitol (sugar alcohol).

Mixtures of carbon and boron sources at different mass ratios were prepared, and the mixtures were weighed such that the total mass of the elements was 5 g. The weight shares, element weights, and weights of the reagents are listed in Table 1.

The weighed mixtures were dissolved in distilled water, placed in Teflon crucibles, and thermally treated at 423 K for 24 h. The resulting products were de-agglomerated by applying ultrasound for 90 s using a Sonics VCX 500 probe (Sonics & Materials Inc., Newtown, CT, USA). A Universal 320R centrifuge (Hettich, Kirchlengern, Germany) was used for particle separation. The centrifugation process was carried out for 30 min (0.5 h), and the number of revolutions per minute was 7000 G. The suspensions were dried via

recrystallization (at 60 °C) and lyophilization (using liquid nitrogen). Differences in the dehydration methods of the boron saccharide precursors affected the degree of the agglomeration of the precursors and the color of the powders obtained. The precursors were placed in graphite crucibles, and boron carbide synthesis was carried out at 1650 °C, with a holding time of 1 h, under a protective atmosphere of argon.

**Table 1.** Weight proportions and masses of reagents.

| Weight Proportions [%] | | Masses of Elements in Precursors [g] | | Weights of Reagents [g] | | | |
|---|---|---|---|---|---|---|---|
| **C** | **B** | **C** | **B** | **Boron Acid** | **Fructose, Glucose** | **Inulin** | **Sorbitol** |
| 50 | 50 | 2.5 | 2.5 | 14.298 | 6.250 | 5.625 | 6.316 |
| 60 | 40 | 3 | 2 | 11.438 | 7.500 | 6.750 | 7.580 |
| 70 | 30 | 3.5 | 1.5 | 8.579 | 8.750 | 7.875 | 8.843 |
| 80 | 20 | 4 | 1 | 5.719 | 10.000 | 9.000 | 10.106 |

The following analyses were carried out to analyze the properties of the products obtained at various stages of the study as well as the mechanisms that controlled the transformation. The suspensions that were the products of the processes described were subjected to a grain size distribution study via dynamic light scattering (DLS) using a Zetasizer Nano (AP Instruments Inc., Santa Rosa, CA, USA). The obtained boron saccharide precursors were analyzed for their chemical bonds using mid-infrared (FT-IR) spectroscopy. A VERTEX 70v spectrophotometer (Bruker, Billerica, MA, USA) was used for this purpose. Both boron–saccharide precursors and synthesis products were observed using an ultra-high-resolution Nova 200 NanoLab scanning electron microscope (FEI Europe, Eindhoven, The Netherlands). An energy dispersive spectroscopy (EDS) analysis was also performed using the built-in attachment for the electron microscope.

## 3. Results

### *3.1. DLS Analysis*

The results of the DLS particle size analysis are summarized in Figure 1 and Table 2. The results in the table show the average grain size and two maxima visible in the graph.

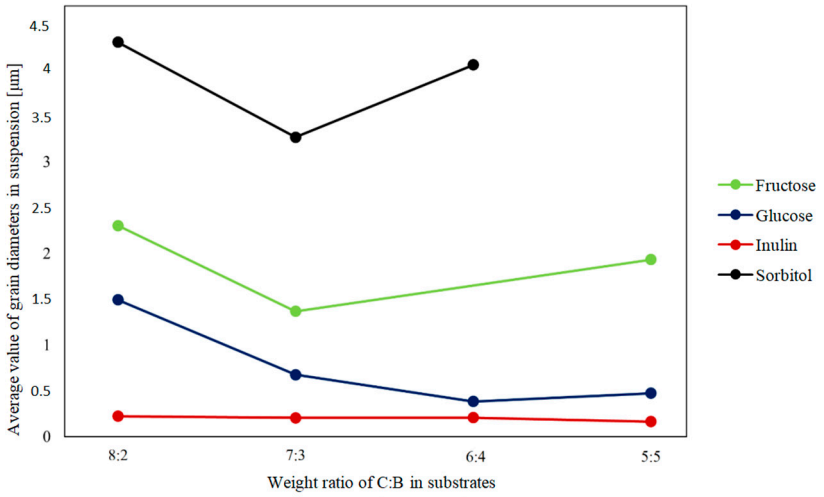


**Figure 1.** DLS analysis results.

**Table 2.** DLS analysis results for each tested sample.

| Sample | Average Grain Size [μm] | Maximum 1 [μm] | Maximum 2 [μm] |
|---|---|---|---|
| F 8:2 | 2.304 | 1.890 | - |
| F 7:3 | 1.369 | 2.225 | 0.197 |
| F 6:4 | 0.208 | 0.227 | 5.076 |
| F 5:5 | 1.933 | 1.881 | - |
| G 8:2 | 1.494 | 1.477 | - |
| G 7:3 | 0.677 | 0.737 | - |
| G 6:4 | 0.384 | 0.419 | 3.531 |
| G 5:5 | 0.475 | 0.546 | - |
| I 8:2 | 0.223 | 0.249 | - |
| I 7:3 | 0.205 | 0.234 | - |
| I 6:4 | 0.208 | 0.222 | 4.844 |
| I 5:5 | 0.164 | 0.170 | 5.271 |
| S 8:2 | 4.306 | 0.770 | - |
| S 7:3 | 3.269 | 1.697 | - |
| S 6:4 | 4.058 | 0.818 | - |
| S 5:5 | 0.38 | 0.165 | 1.475 |

The samples are labelled as follows: the letter indicates the saccharide name, and the numbers indicate the proportion of carbon:boron (for example, F 8:2 indicates a sample containing fructose with 80% carbon and 20% boron).

From the results in Table 2, it can be concluded that the grain-size distribution in the samples was mostly unimodal. The values included in the "Maximum 1" column refer to peaks with intensities greater than 95%. In some samples, the presence of a second peak was registered, but its presence and intensity were due to the presence of fractions that had not been broken down by centrifugation or ultrasound action (they can be considered as impurities).

Figure 1 shows the dependence of the particle size in suspension on the ratio of carbon to boron (C:B) in the prepared precursor mixtures. In samples containing inulin and glucose prior to hydrothermal treatment, a decrease in the average grain size was noticeable as the proportion of boron increased, whereas for the other samples, this relationship was apparent only for samples containing more than 60 wt.% carbon, and the highest average grain size was recorded for the samples in which the precursor was sorbitol. Figure 1 does not show the results for samples F 6:4 and S 5:5, due to the more than tenfold difference in the values obtained during the measurement in relation to the rest of the samples containing the same carbon source.

### *3.2. FT-IR Analysis*

Spectrophotometric measurements of the tested samples were performed, and FT-IR spectra were obtained. Both the recrystallized and freeze-dried precursors were studied, the obtained spectra were analyzed, and the characteristic bands were marked using available databases. The influence of the method of dehydrating suspensions, which are the products of hydrothermal treatment, on the chemical composition of the precursors obtained was analyzed.

FT-IR spectra for two different precursors (glucose and sorbitol) for two dehydration methods are presented; analogous spectra were obtained and analyzed. From the graphs (Figures 2–5), the repeatability of the absorption bands in almost all spectra was noted. The positions of the bands were independent of the weight ratios of the substrates involved in the reactions under hydrothermal conditions, whereas their intensities changed, indicating

the similarity of the products obtained at this stage of the research. Distinctly different from the others are the spectra of sorbitol, which may indicate a different reaction mode. Based on the literature data [4,5], Table 3 was prepared, in which the interpretations of bands visible on the obtained spectra are provided.

**Table 3.** Wavelengths with meanings for FT-IR analysis.

| Wave Number [cm$^{-1}$] | Meaning |
|---|---|
| 3392–3398 | The band corresponds to an intramolecular, stretching O–H bond |
| 3215 | The band characteristic of boronic acid corresponds to an intramolecularly stretched O–H bond |
| 2929–2950 | The band corresponds to astretching C–H bond, characteristic of alkanes |
| 2518–2520 | The band corresponds to the tensile O–H bond |
| 2362 | The band corresponds to the O=C=O group |
| 2262 | The band corresponds to a stretching C≡C bond |
| 1707 | The band corresponds to a C=O stretching bond, characteristic of an aldehyde or ketone group |
| 1620–1636 | The band corresponds to a stretching C=C bond |
| 1434–1457 | The band characteristic of boric acid |
| 1194–1195 | |
| 970–1027 | The band characteristic of glucose |
| 883 | The band corresponds to the deformation bond C=C |
| 805–814 | The band characteristic of the HC=CH group belonging to the five-atom ring |
| 643–651 | The band characteristic of the furan ring |

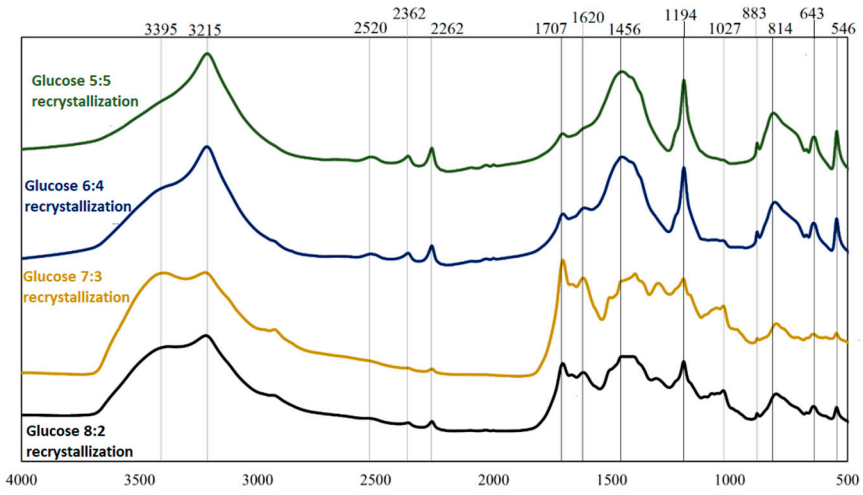


**Figure 2.** FT-IR spectra for boron–saccharide precursors after hydrothermal treatment, obtained via recrystallization with glucose as a carbon source.

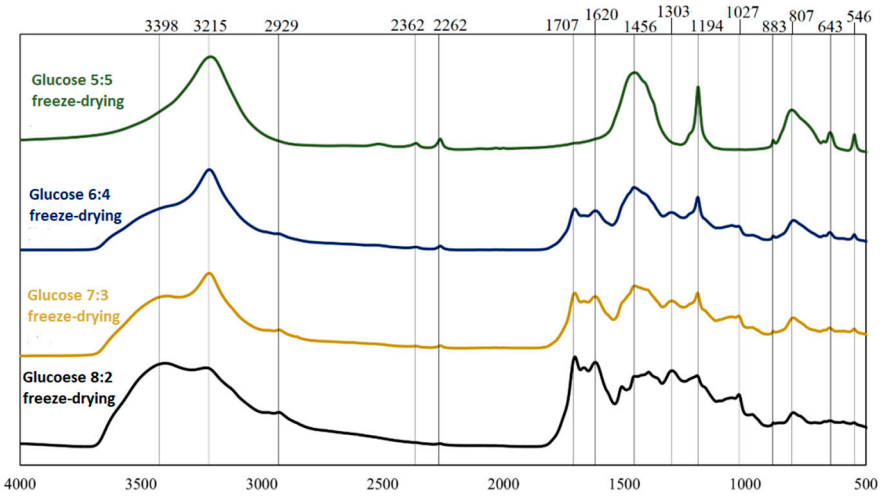


**Figure 3.** FT-IR spectra for boron–saccharide precursors after hydrothermal treatment, obtained via freeze-drying with glucose as a carbon source.

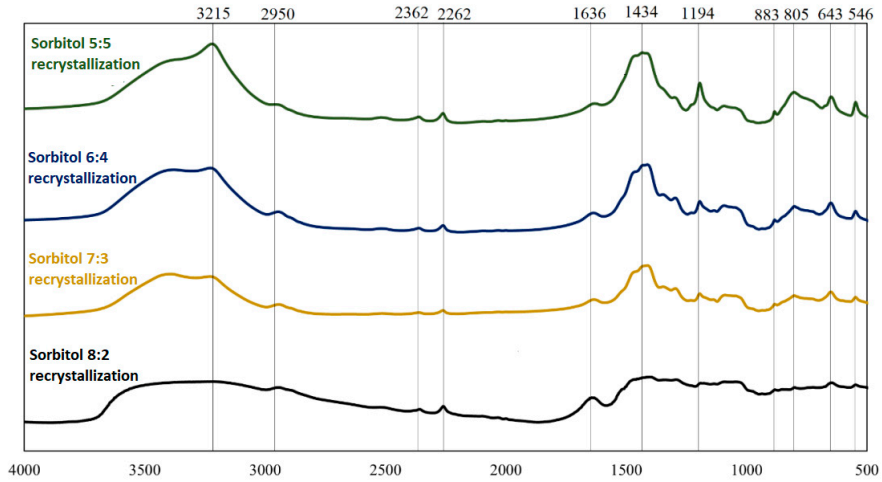


**Figure 4.** FT-IR spectra for boron–saccharide precursors after hydrothermal treatment, obtained via recrystallization with sorbitol as a carbon source.

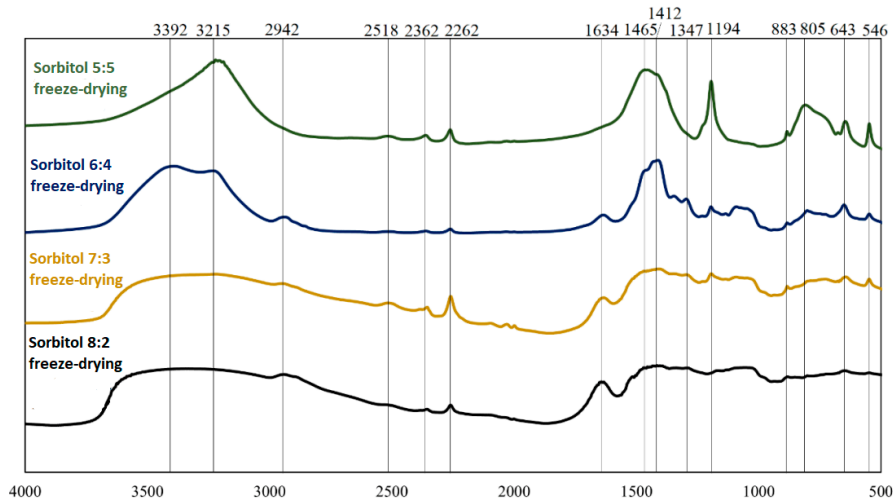


**Figure 5.** FT-IR spectra for boron–saccharide precursors after hydrothermal treatment, obtained via freeze-drying with sorbitol as a carbon source.

An analysis of the spectra in which inulin and fructose were the precursors revealed that they were identical in terms of spectral position (both precursors were ketoses). Comparing the precursors formed using saccharides belonging to different groups (aldoses and ketoses), it can be concluded that the products obtained are qualitatively similar. However, the proportions of the individual chemical bond types and elemental groupings were not similar, as indicated by the different intensities of the corresponding bands. Significant differences were observed in the spectra of sorbitol. The observation of bands corresponding to bonds between oxygen and hydrogen, carbon and hydrogen, and oxygen and carbon indicates that the reactants did not completely decompose during hydrothermal treatment. The 814 $cm^{-1}$ and 643 $cm^{-1}$ bands confirm the presence of HMF in the boron–saccharide precursors obtained.

### *3.3. SEM Images for Precursors*

The figures below show SEM images taken with a Nova 200 NanoLab scanning electron microscope (SEM) from FEI Europe Company with an integrated EDS unit. From the images shown in Figure 6, it can be seen that the spheres formed during the hydrothermal treatment of glucose are characterized by a smaller grain size than in the case of fructose. In the images of the samples with a boron content of less than 50% in the precursor, only spherical structures are visible and not deformed, but aggregation and agglomeration are observed. In the case of a sample with a carbon-to-boron weight ratio of 7:3, the bi-modality of the precursor grain size distribution was noted. Particles of boric acid were visible only in the case of the sample with an equal weight ratio of carbon to boron.

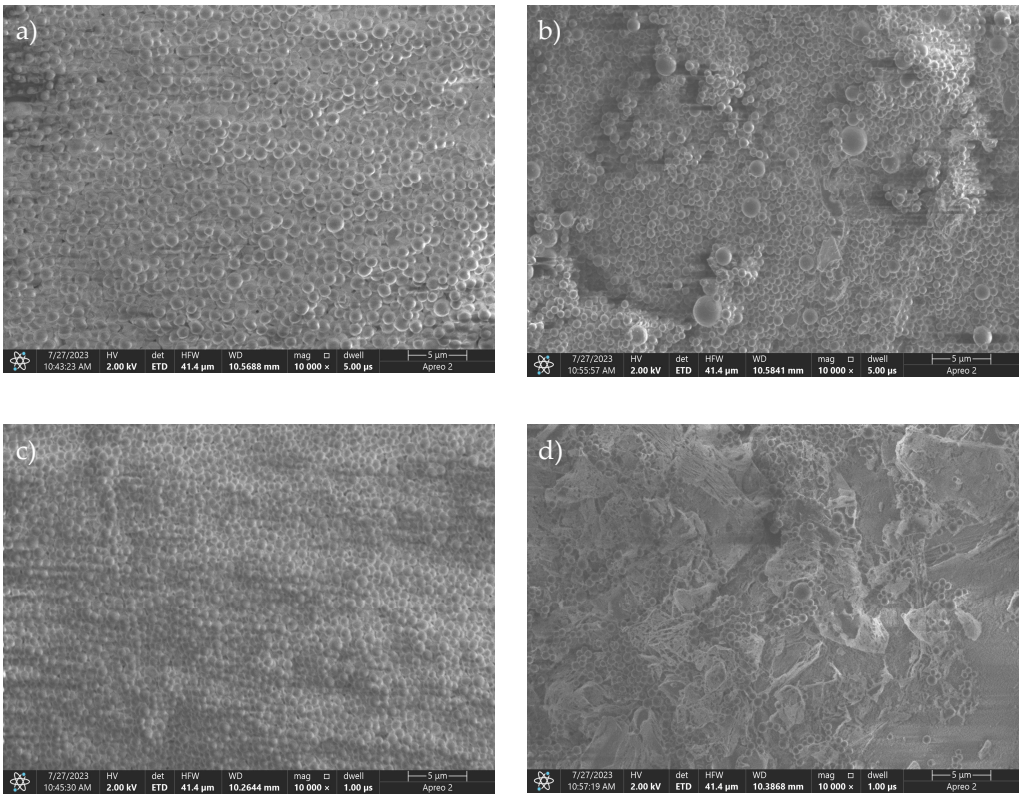


**Figure 6.** SEM images of the saccharide precursors obtained using the hydrothermal method from glucose and dried via recrystallization. Weight ratios of carbon to boron: (**a**) 8:2, (**b**) 7:3, (**c**) 6:4, (**d**) 5:5.

The microstructure images produced via SEM analysis (Figure 7) show that freeze-drying affected the morphology of the product (the same was true for other sugars, e.g., fructose). The sample with a low boron content was morphologically very similar to its counterpart dried via recrystallization. Samples 7:3 and 6:4 were characterized by a significant agglomeration of carbon spheres with boric acid in between. The image of the sample

with the highest boron content shows sparse carbon spheres within the boric acid matrix. The pronounced bi-modality of the grain size distribution was attributed to the precursor obtained using the hydrothermal treatment of a mixture of glucose and boric acid with carbon-to-boron ratios of 7:3 by weight.

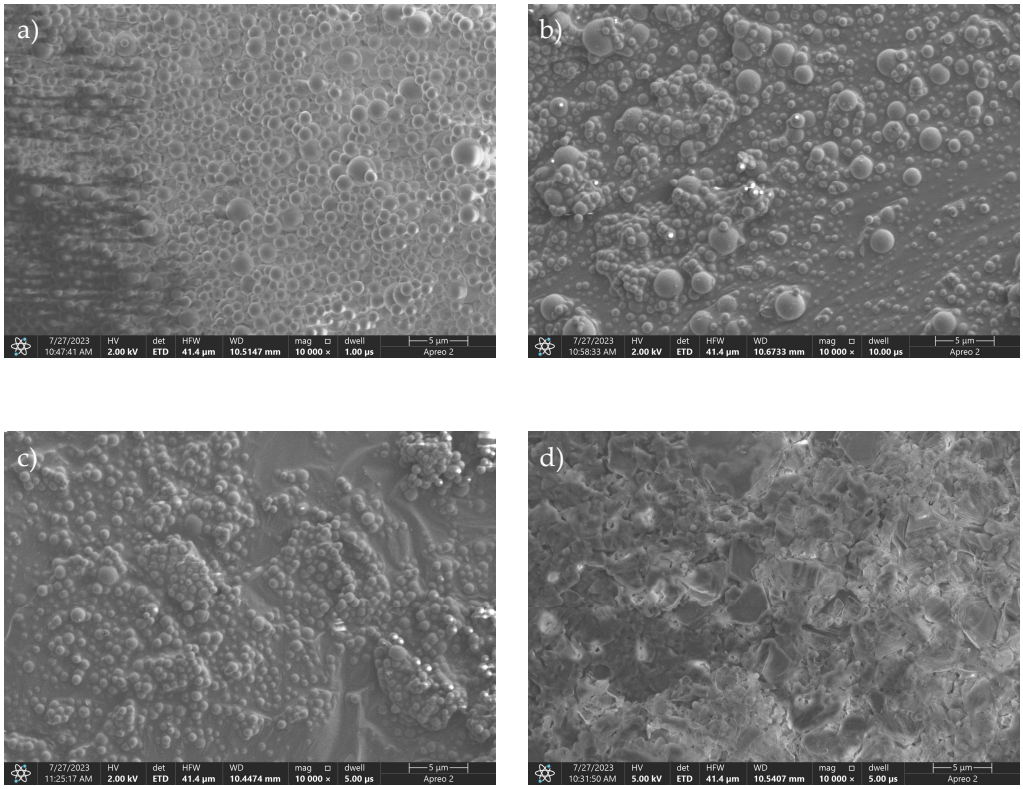


**Figure 7.** SEM images of the saccharide precursors obtained using the hydrothermal method from glucose and freeze-dried. Weight ratios of carbon to boron: (**a**) 8:2, (**b**) 7:3, (**c**) 6:4, (**d**) 5:5.

The SEM images shown in Figure 8 are significantly different from all the boron–saccharide precursor photographs shown above. The presence of carbon spheres, which is characteristic of the hydrothermal treatment of saccharides, is not clearly observed. The consistency of the product obtained after recrystallization resembled that of a glassy polymer. The organic nature of the obtained precursors was confirmed by the dark traces visible in the photograph of sample 8:2, which are areas burnt off under electron microscopy. As the proportion of boron to carbon increased, crystallites of boric acid could be seen on the surface of the polymer.

As shown in Figure 9, the freeze-drying process affected the morphology of the resulting product, regardless of the precursor used. Boric acid is visible in the SEM images. Powders with a weight proportion of carbon greater than 50% obtained via freeze-drying immediately absorbed the water present in the air when removed from the vacuum. Samples with a high proportion of carbon were characterized by the consistency of liquids with very high viscosities.

Based on the analyses presented above, a graph comparing the particle sizes of the precursors before and after the dehydration process (considering both possible recrystallization and dehydration processes) was plotted.

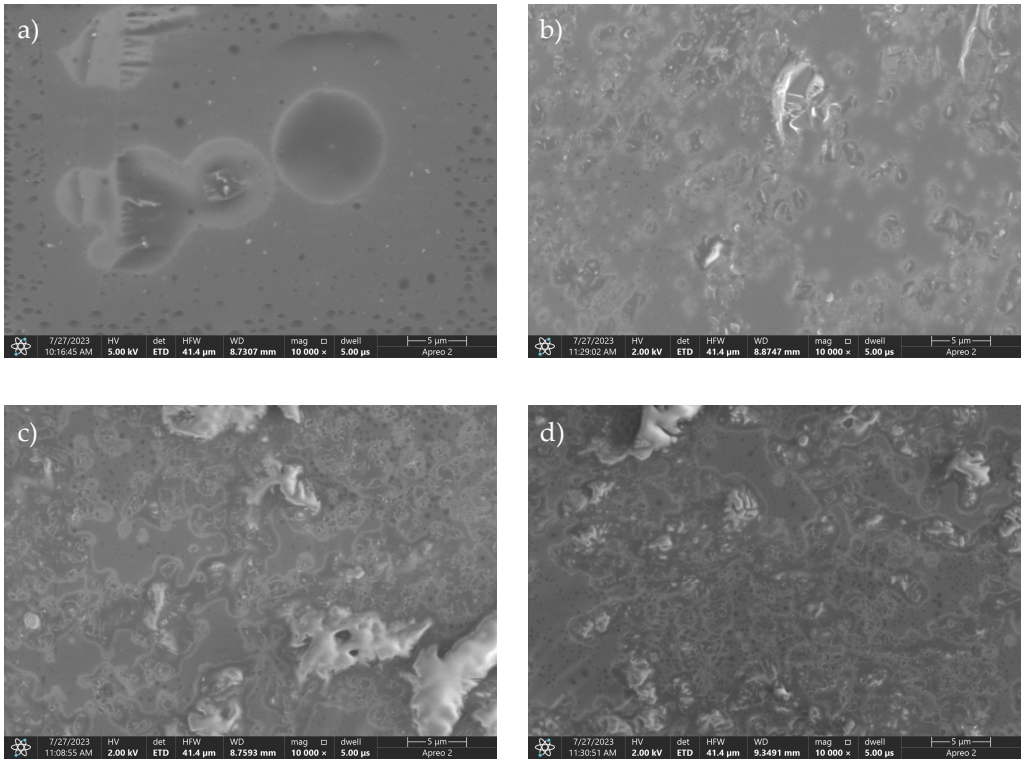


**Figure 8.** SEM images of the saccharide precursors obtained using the hydrothermal method from sorbitol and dried via recrystallization. Weight ratios of carbon to boron: (**a**) 8:2, (**b**) 7:3, (**c**) 6:4, (**d**) 5:5.

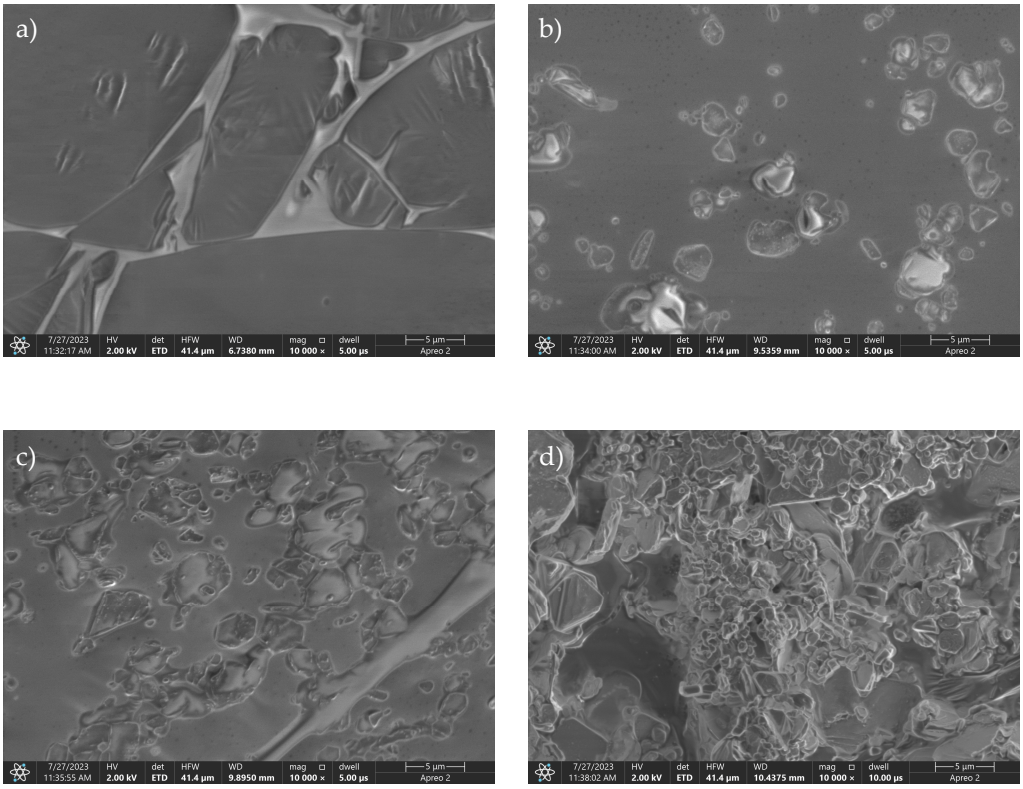


**Figure 9.** SEM images of the saccharide precursors obtained using the hydrothermal method from sorbitol and freeze-dried. Weight ratios of carbon to boron: (**a**) 8:2, (**b**) 7:3, (**c**) 6:4, (**d**) 5:5.

The data shown in Figure 10 demonstrate that the dehydration process, carried out both via freeze-drying and recrystallization, affected the particle size of the boron–saccharide precursors for samples in which polysaccharide inulin was the carbon source. The diameter of the inulin precursor after water removal was 40 times that of the particles in the suspension, indicating that spherical precursor particles with diameters of 4–8 µm were agglomerates of smaller spheres with diameters of approximately 0.2 µm.

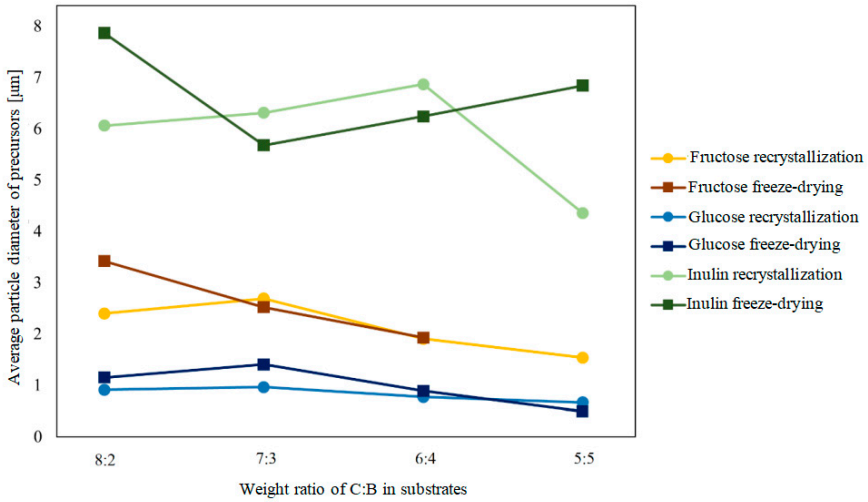


**Figure 10.** Comparison of precursor particle sizes before and after dehydration.

### *3.4. SEM Images for Final $B_4C$ Product*

B4C powders were produced using the boron–saccharide precursors under investigation according to the procedure described above. After sintering, the samples were prepared for electron microscope (SEM) observation by performing the necessary steps.

The SEM images shown in Figure 11 show a change in the morphology of the resulting $B_4C$ powders with changing C:B ratios. A visible change was observed in the morphology of the powder with a 7:3 ratio (Figure 11b) compared with thatin the sample with a 6:4 ratio (Figure 11c). The grain morphology was different in the images of the samples with the highest proportion of carbon in the precursor. At a lower boron proportion, particles that are aggregates of plate-shaped grains are visible. For samples with the highest proportion of boron, the grains had a near-spherical shape (Figure 11a). The size of the microstructural elements increased as the proportion of carbon in the precursors decreased. Based on EDS analysis, the large particles visible in the image (Figure 11d) were partly composed of boron carbide. The SEM images show the interior of the particles, and their micro structures were clearly porous. The pores were spherical in shape. The recorded proportion of carbon (greater than 20%) suggests that none of the precursors that build large grains reacted.

The SEM images shown in Figure 12 provide evidence that as the proportion of boron in the reaction mixture increases, there is a gradual agglomeration of the precursors, followed by are action between boron and carbon. A particle form different from the spherical form was visible only in the case of the sample with the highest boron content. EDS analysis showed that only particle “I” in Figure 12d is made of boron carbide, while structure “II” is an agglomerate of unreacted precursors.

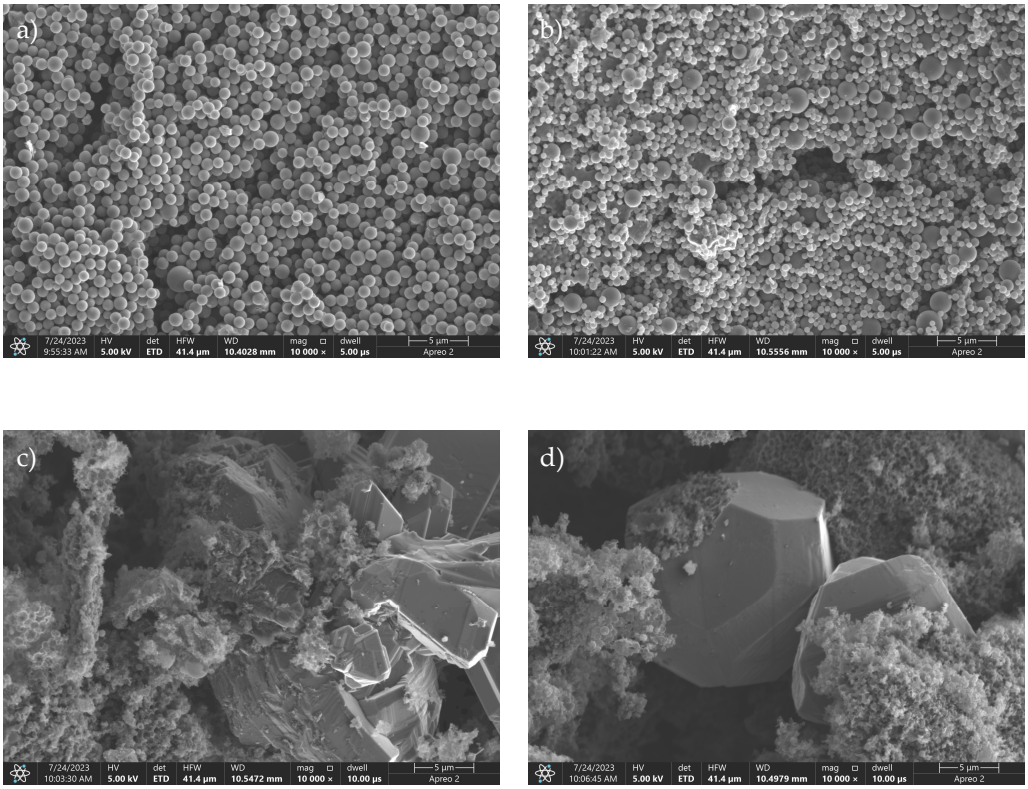


**Figure 11.** SEM images of boron carbide powders produced from a glucose precursor dried via recrystallization. Weight ratios of carbon to boron: (**a**) 8:2, (**b**) 7:3, (**c**) 6:4, (**d**) 5:5.

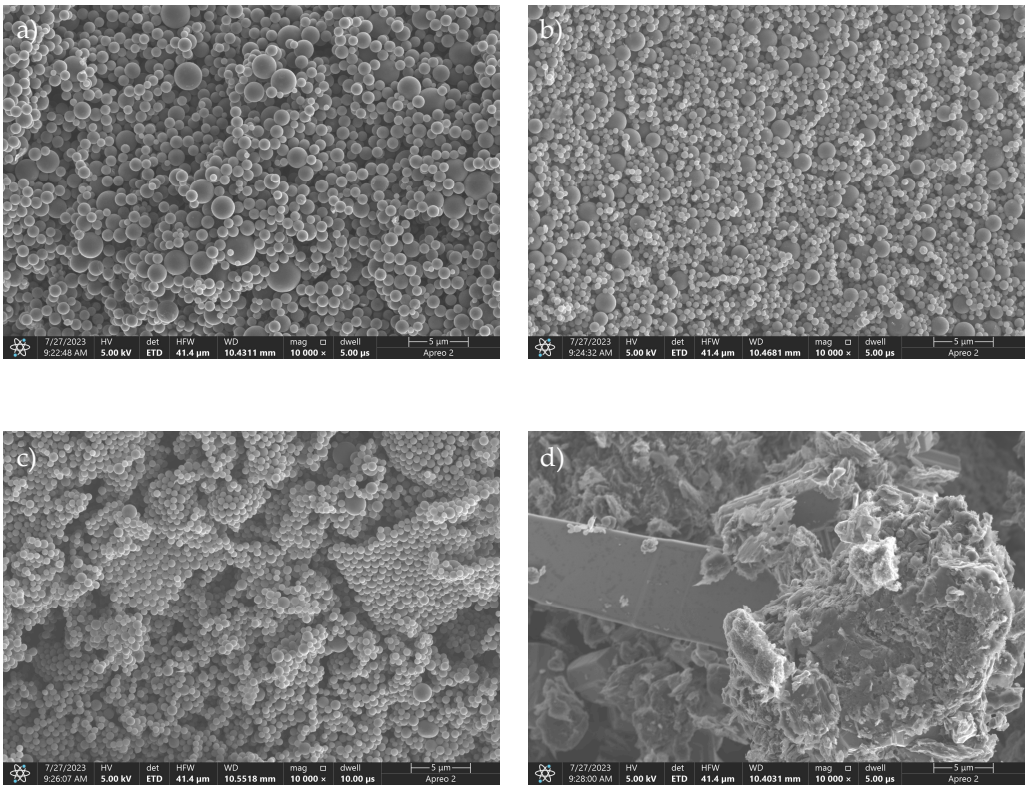


**Figure 12.** SEM images of boron carbide powders produced from a glucose precursor via freeze-drying. Weight ratios of carbon to boron: (**a**) 8:2, (**b**) 7:3, (**c**) 6:4, (**d**) 5:5.

The SEM images shown in Figure 13 show that precursors containing sorbitol as a carbon source for as low as 20 wt% boron allowed the boron carbide formation reaction to occur. The grains were composed of agglomerates of lamellar particles with dimensions that increased with increasing boron content in the reaction mixture. For samples with a boron content of less than 40%, areas of morphology significantly different from lamellae, which are boron carbide grains, were visible. For samples in which the boron content in the precursor exceeded 30%, only crystallites could be seen in the SEM images. EDS analysis showed that for the sorbitol precursors, the formation of $B_4C$ occurred independently of the C:B ratio in the synthesis substrate.

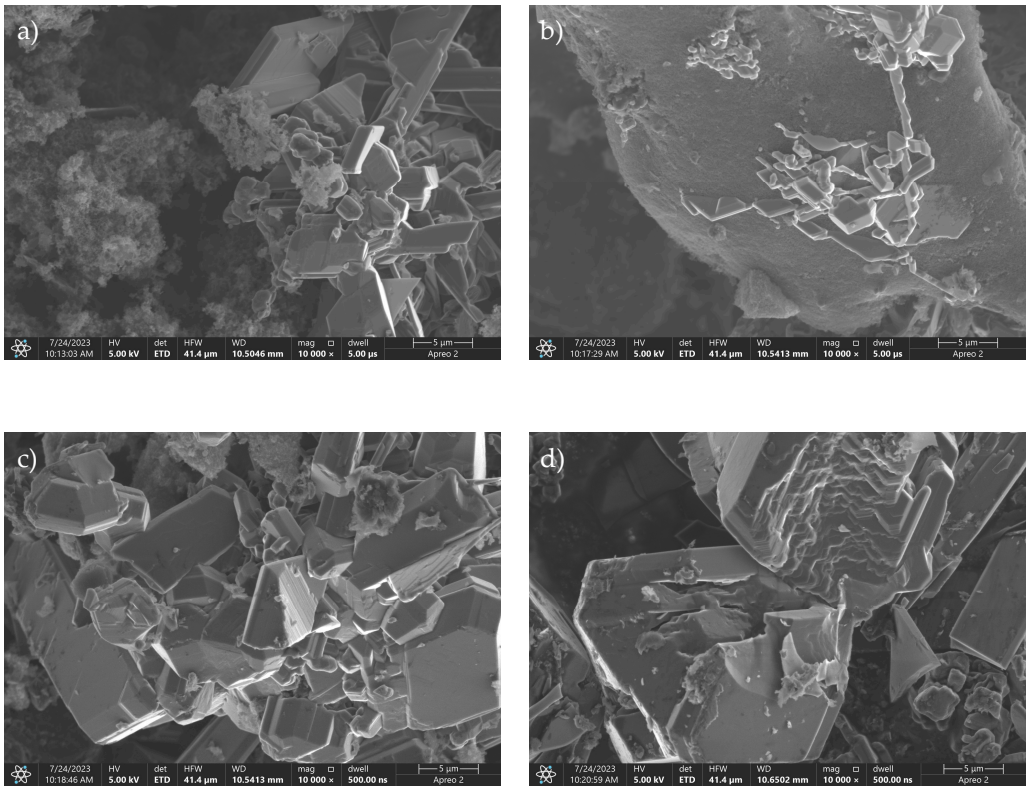


**Figure 13.** SEM images of boron carbide powders produced from a sorbitol precursor dried via recrystallization. Weight ratios of carbon to boron: (**a**) 8:2, (**b**) 7:3, (**c**) 6:4, (**d**) 5:5.

The SEM images shown in Figure 14 prove that sorbitol precursors allow boron carbide to be obtained at low boron-weight shares. The effect of freeze-drying as a method of precursor dehydration on their morphology is not clear. Samples with C:B ratios of 6:4 and 7:3 showed particles with larger dimensions than those obtained using recrystallized precursors. The sample with the highest boron content, on the other hand, was characterized by significantly smaller platelet dimensions compared to a sample of identical composition not subjected to freeze-drying. The platelets were elongated and formed agglomerates, and EDS analysis showed a different trend (compared with the other cases studied). The sample containing the highest amount of boron in the precursor after synthesis contained only 25% boron in the area capable of forming a boron carbide crystallite. The boron content characteristic of the boron carbide homogeneity range, on the other hand, was characterized by a sample with 80% the weight of carbon atoms in the precursor.

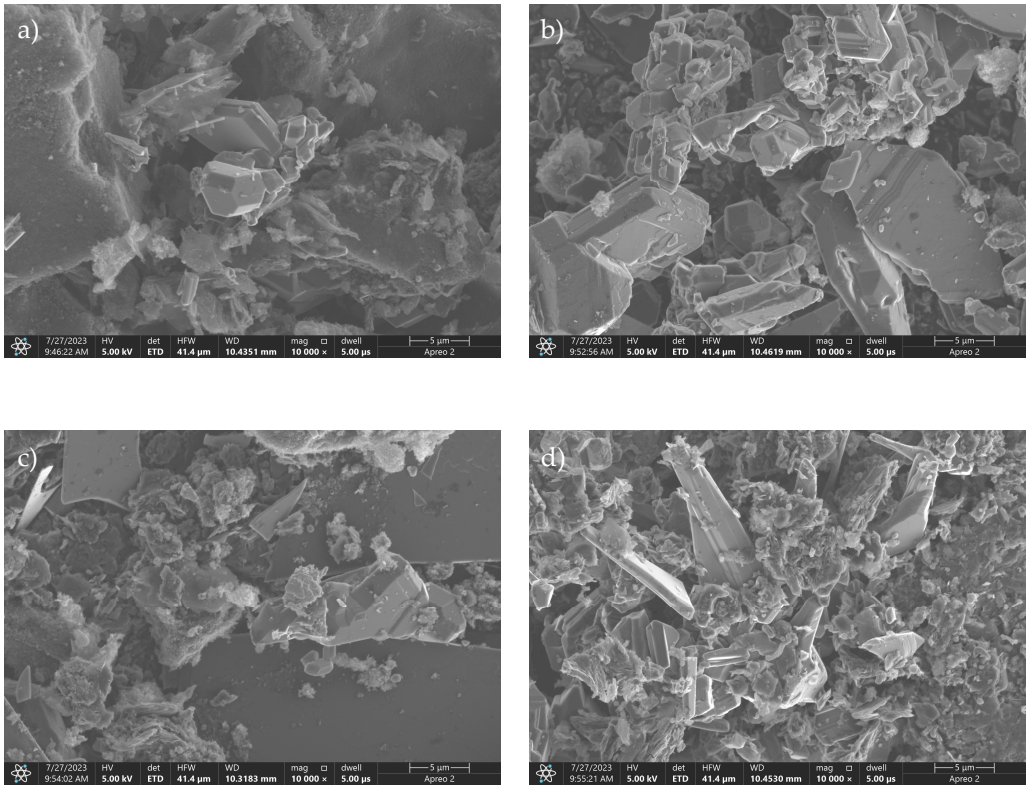


**Figure 14.** SEM images of boron carbide powders produced from a sorbitol precursor via freeze-drying. Weight ratios of carbon to boron: (**a**) 8:2, (**b**) 7:3, (**c**) 6:4, (**d**) 5:5.

## 4. Discussion

The aim of the above work was to synthesize boron carbide with a spherical shape and nanometer-sized grains from boron–saccharide precursors, in which the carbon source was saccharides. The study proved that the type of functional group in a saccharide or its derivative has a significant effect on the size of the spherical grains obtained when saccharides are used. The use of sorbitol does not allow the precursor to be obtained in powder form. Replacing recrystallization in the precursor preparation process with freeze-drying allows for better control of the precursor composition and can also have an impact on reducing the segregation of boron from carbon, which has a key effect on maintaining the spherical shape of grains after the synthesis stage. The results of the FT-IR analysis showed that regardless of the carbon source used, the infrared spectral materials obtained had a similar course, with the exception being the use of sorbitol.

The determined average values of the precursor grain sizes showed that as the proportion of carbon decreased, the average grain size decreased for samples with fructose and sorbitol precursors. In addition, the use of sorbitol as a precursor resulted in grain sizes that were significantly larger (more than double on average) than those of other precursors.

Based on SEM analysis and DLS measurements, it was concluded that the sorbitol precursor exhibited a different powder morphology. The obtained carbon source, as well as the final $B_4C$ powder, was characterized by significantly different parameters from the other tested samples; the grain size was much larger, and the SEM images showed the absence of spherical phases present in the other tested materials. This is related to the structure of sorbitol, in which there are hydroxyl groups on both sides of the carbon chain; therefore, the polycondensation step cannot occur. The sorbitol precursors after the dehydration stage differed significantly from the others. The recrystallized samples resembled a glassy polymer in terms of consistency; freeze-dried samples were liquids with very high viscosity.

SEM images of the samples with other boron–saccharide precursors showed the presence of spherical grains. For these samples, as the proportion of boron increased,

a decrease in the proportion of spherical grains was observed, whereas the number of lamellar and irregular grains increased. For glucose and fructose precursors at high carbon shares, a structure with a large number of spherical grains was observed, and irregular grains began to appear only for carbon shares lower than 70%.

According to theoretical assumptions, the size of the boron carbide grains was much larger than that of the precursor grains. Based on the DLS analysis, the smallest grain sizes characterized the inulin precursors; however, each of the two dehydration processes involved grain agglomeration, which affected the glucose and fructose precursors much less than those in which the polysaccharide was the carbon source. By varying the ratio of carbon to boron during precursor preparation, the stoichiometry of boron carbide can be controlled. Boron carbide, rich in boron, was obtained at a C:B ratio of 5:5. For carbon ratios in the 60–70% range, boron carbide, rich in boron, or metastable $BC_5$ and $BC_7$ phases were obtained, depending on the saccharide used and the dehydration method. For a carbon-to-boron ratio of 8:2, boron carbide with a $B_4C$ stoichiometry and the aforementioned metastable phases were obtained. The results demonstrate the progress of work on the synthesis of boron carbide from saccharide precursors.

## 5. Conclusions

- Boron–saccharide precursors were obtained using a hydrothermal method where the carbon source was saccharides or their derivatives (glucose, fructose, inulin, and sorbitol).
- The functional group in a saccharide or its derivative has a significant effect on the size of the spherical grains obtained when saccharides are used.
- Due to the structure of sorbitol, its use as a carbon source resulted in the formation of a saccharide precursor and ultimately a boron carbide with a morphology different from that of other compounds as carbon sources.
- The smallest grain sizes characterized inulin precursors, but each of the two dehydration processes involved grain agglomeration, and glucose precursors and fructose precursors were much less affected than those in which the carbon source was a polysaccharide.
- The use of glucose, fructose, and inulin makes it possible to obtain precursors that are similar in terms of their chemistry but differ significantly in terms of powder morphology.
- The freeze-drying process had no significant effect on the composition of the precursors, but SEM analysis showed that it caused a change in the morphology of the precursors compared to recrystallized samples.
- $B_4C$ powder with a high proportion of spherical grains for glucose and fructose precursors was obtained at high proportions of carbon (above 70%).
- The use of sorbitol as a carbon source resulted in the formation of boron carbide with non-spherical grain shapes.
- Failed to produce nanometer-sized grains of boron carbide.

**Author Contributions:** Conceptualization, D.K., K.P., W.B. and M.Z.; Methodology, D.K. and K.P.; Formal analysis, D.K., K.P., W.B. and M.Z.; Investigation, W.B. and M.Z.; Data curation, K.P. and J.P.; Writing—original draft, D.K.; Writing—review and editing, D.K., K.P., W.B., M.Z. and J.P.; Visualization, D.K. and K.P.; Supervision, J.P. All authors have read and agreed to the published version of the manuscript.

**Funding:** This research was funded by the National Science Center, Poland (grant no. DEC-2021/05/X/ST8/01051).

**Data Availability Statement:** The data presented in this study are available on request from the corresponding author.

**Conflicts of Interest:** The authors declare no conflicts of interest.

## References


1. Cheng, C.; Reddy, K.M.; Hirata, A.; Fujita, T.; Chen, M. Structure and mechanical properties of boron-rich boron carbides. *J. Eur. Ceram. Soc.* **2017**, *37*, 4514–4523. [CrossRef]
2. Kovalev, D.Y.; Konovalihin, S.V. Boron Carbide. In *Concise Encyclopedia of Self-Propagating High-Temperature Synthesis*; Elsevier Inc.: Amsterdam, The Netherlands, 2017. [CrossRef]
3. Gubernat, A.; Pichór, W.; Zientara, D.; Bućko, M.M.; Zych, Ł.; Kozień, D. Direct synthesis of fine boron carbide powders using expanded graphite. *Ceram. Int.* **2019**, *45*, 22104–22109. [CrossRef]
4. Zhang, W.; Yamashita, S.; Kita, H. Progress in pressureless sintering of boron carbide ceramics—A review. *Adv. Appl. Ceram.* **2019**, *118*, 222–239. [CrossRef]
5. Gosset, D. Basic Properties of Boron Carbide. In *Comprehensive Nuclear Materials*, 2nd ed.; Elsevier: Amsterdam, The Netherlands, 2020; pp. 539–553. [CrossRef]
6. Kozien, D. Autoreferat "Synteza i Określenie Właściwości Biologicznych". Ph.D. Thesis, AGH University of Science and Technology, Kraków, Poland, 2021; pp. 1–30.
7. Kozien, D.; Szermer-Olearnik, B.; Rapak, A.; Szczygieł, A.; Anger-Góra, N.; Boratynski, J.; Pajtasz-Piasecka, E.; Bucko, M.M.; Pedzich, Z. Boron-rich boron carbide nanoparticles as a carrier in boron neutron capture therapy: Their influence on tumor and immune phagocytic cells. *Materials* **2021**, *14*, 3010. [CrossRef]
8. Alizadeh, A.; Taheri-Nassaj, E.; Ehsani, N. Synthesis of boron carbide powder by a carbothermic reduction method. *J. Eur. Ceram. Soc.* **2004**, *24*, 3227–3234. [CrossRef]
9. Gao, S.; Li, X.; Wang, S.; Xing, P.; Kong, J.; Yang, G. A low cost, low energy, environmentally friendly process for producing high-purity boron carbide. *Ceram. Int.* **2019**, *45*, 3101–3110. [CrossRef]
10. Riman, R.E. Powders, Solution Synthesis of. In *Encyclopedia of Materials: Science and Technology*; Elsevier: Amsterdam, The Netherlands, 2001; pp. 7800–7811. [CrossRef]
11. Li, D.; Yao, J.; Wang, H. Hydrothermal synthesis of $AlPO_4$-5: Effect of precursor gel preparation on the morphology of crystals. *Prog. Nat. Sci. Mater. Int.* **2012**, *22*, 684–692. [CrossRef]
12. Zheng, F.; Liu, H.; Liu, D.; Yao, S.; Yan, T.; Wang, J. Hydrothermal and wet-chemical synthesis of pure $LiTaO_3$ powders by using commercial tantalum hydroxide as starting material. *J. Alloys Compd.* **2009**, *477*, 688–691. [CrossRef]
13. Mohan, S.; Vellakkat, M.; Aravind, A.; Reka, U. Hydrothermal synthesis and characterization of Zinc Oxide nanoparticles of various shapes under different reaction conditions. *Nano Express* **2020**, *1*, 030028. [CrossRef]
14. Seal, M.; Mukherjee, S. Determination of hydrothermal synthesis pressure of crystalline $GeO_2$ nano particle of the order of 10 nm through a Central Force Potential model. *Mater. Today Proc.* **2018**, *5*, 10169–10176. [CrossRef]
15. Feng, S.H.; Li, G.H. Hydrothermal and Solvothermal Syntheses. In *Modern Inorganic Synthetic Chemistry*; Elsevier: Amsterdam, The Netherlands, 2017. [CrossRef]
16. Khan, L.; Khan, Z. Bifunctional Nanomaterials: Magnetism, Luminescence and Multimodal Biomedical Applications. In *Complex Magnetic Nanostructures: Synthesis, Assembly and Applications*; Springer: Cham, Switzerland, 2017; pp. 121–171. [CrossRef]
17. Kozień, D.; Jeleń, P.; Sitarz, M.; Bucko, M. Synthesis of boron carbide powders from mono- and polysaccharides. *Int. J. Refract. Met. Hard Mater.* **2019**, *86*, 105099. [CrossRef]
18. Devi, H.V.S.; Swapna, M.S.; Raj, V.; Ambadas, G.; Sankararaman, S. Natural cotton as precursor for the refractory boron carbide—A hydrothermal synthesis and characterization. *Mater. Res. Express* **2018**, *5*, 15603. [CrossRef]
19. SarithaDevi, H.V.; Swapna, M.S.; Ambadas, G.; Sankararaman, S. Low-temperature green synthesis of boron carbide using aloe vera. *Chin. Phys. B* **2018**, *27*, 107702. [CrossRef]
20. Sudoh, A.; Konno, H.; Habazaki, H.; Kiyono, H. Synthesis of boron carbide microcrystals from saccharides and boric acid. *Tanso* **2007**, *2007*, 8–12. [CrossRef]
21. Shao, Y.; Lu, W.; Meng, Y.; Zhou, D.; Zhou, Y.; Shen, D.; Long, Y. The formation of 5-hydroxymethylfurfural and hydrochar during the valorization of biomass using a microwave hydrothermal method. *Sci. Total Environ.* **2021**, *755*, 142499. [CrossRef] [PubMed]
22. Sevilla, M.; Fuertes, A.B. Chemical and Structural Properties of Carbonaceous Products Obtained by Hydrothermal Carbonization of Saccharides. *Chem.-Eur. J.* **2009**, *15*, 4195–4203. [CrossRef] [PubMed]
23. Kuang, X.; Carotenuto, G.; Nicolais, L. Review of ceramic sintering and suggestions on reducing sintering temperatures. *Adv. Perform. Mater.* **1997**, *4*, 257–274. [CrossRef]
24. Zhang, M.; Yang, H.; Liu, Y.; Sun, X.; Zhang, D.; Xue, D. First identification of primary nanoparticles in the aggregation of HMF. *Nanoscale Res. Lett.* **2012**, *7*, 38. [CrossRef] [PubMed]
25. Available online: https://spectrabase.com/10.08.2023r (accessed on 20 December 2023).


**Disclaimer/Publisher's Note:** The statements, opinions and data contained in all publications are solely those of the individual author(s) and contributor(s) and not of MDPI and/or the editor(s). MDPI and/or the editor(s) disclaim responsibility for any injury to people or property resulting from any ideas, methods, instructions or products referred to in the content.